

Liu et al., <https://doi.org/10.1083/jcb.201611088>

Figure S1. Efficiency of *Tango1* knockdown. Confocal images of wild-type and *Cg>Tango1ⁱ*, where *Tango1* has been knocked down with two different constructs. *Tango1* expression was visualized with anti-*Tango1* antibody staining.

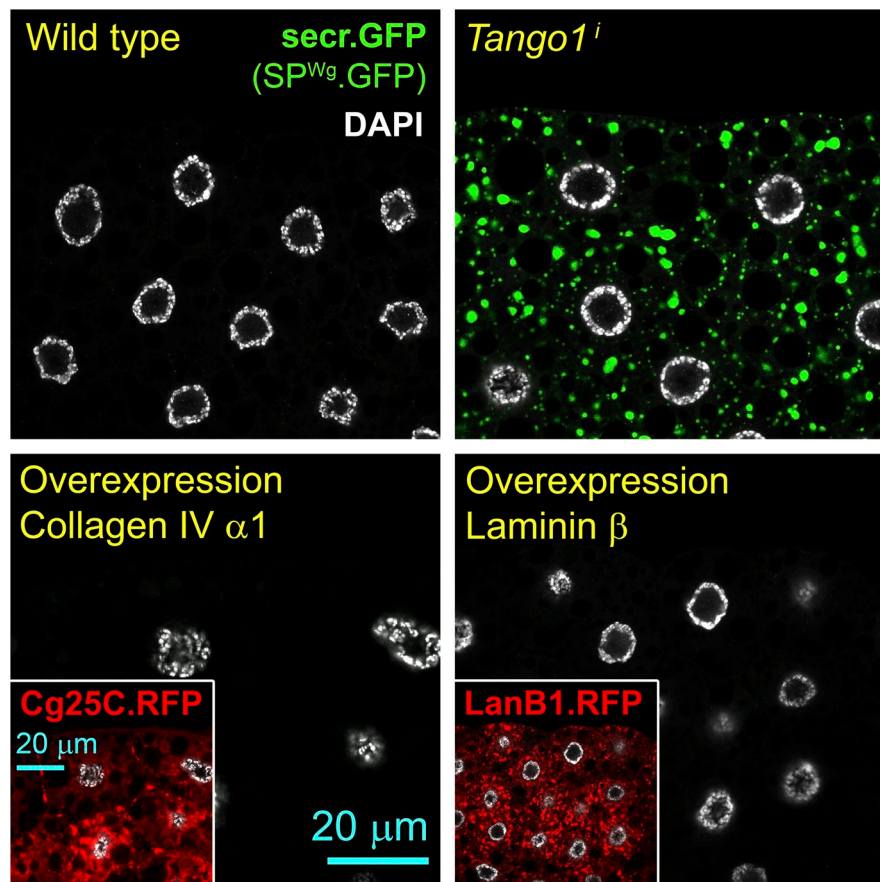


Figure S2. Overexpression of Collagen IV or Laminin single chains does not impair general secretion. Fat body cells expressing secreted GFP under control of BM-40-SPARC-GAL4 (*BM-40-SPARC>secr.GFP*, green). Images are of wild-type fat body, *Tango1ⁱ* fat body, and fat body overexpressing Collagen IV α 1 chain (Cg25C.RFP) and Laminin β chain (LanB1.RFP).

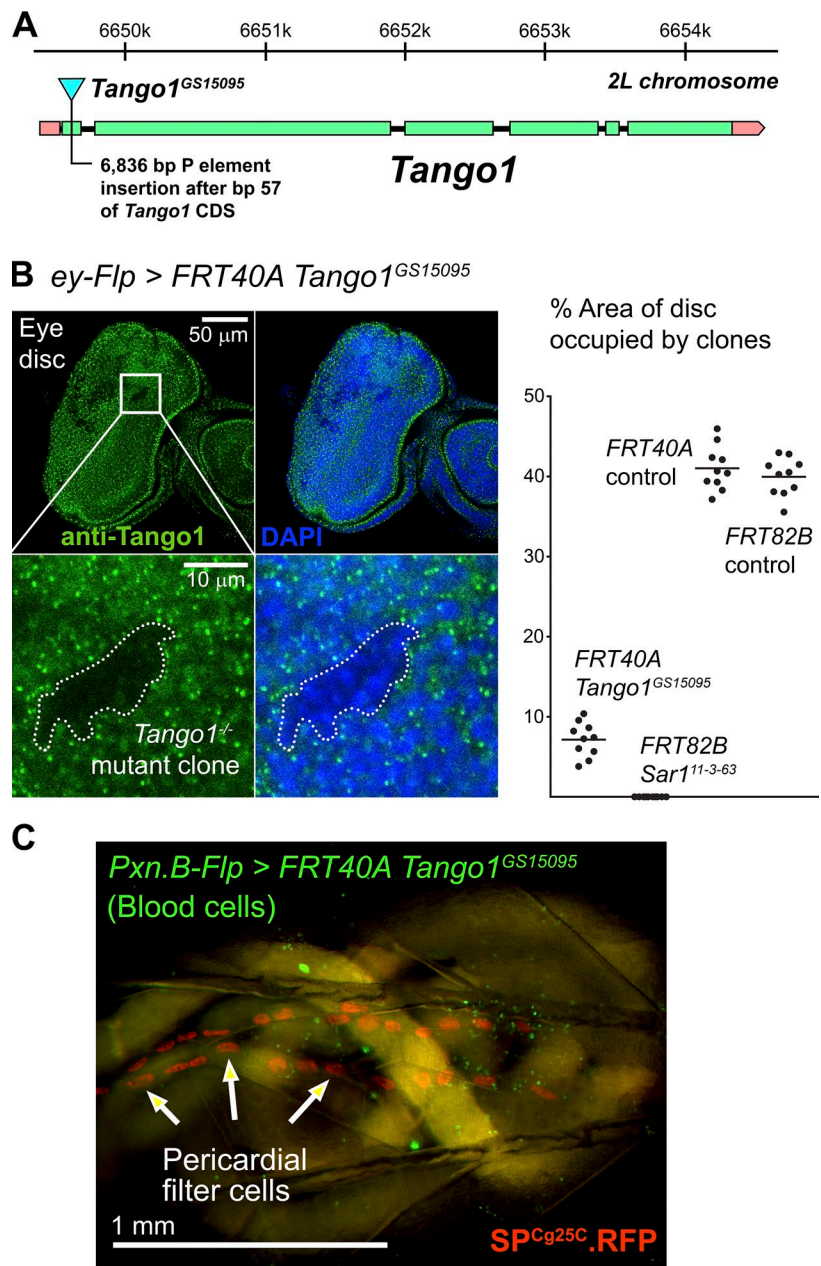


Figure S3. Analysis of *Tango1* mutant mosaics. (A) Graphic representation of the genomic organization of the *Tango1* gene and *Tango1^{GS15095}* mutation caused by a transposon insertion into the first coding exon of the gene. (B) Confocal image of an eye disc showing clones of *FRT40A Tango1^{GS15095}* homozygous mutant cells (absence of *Tango1* antibody staining). Unlike *FRT82B Sar1¹¹¹⁻³⁻⁶³* clones, *FRT40A Tango1^{GS15095}* clones can be recovered but show reduced viability, as indicated by the reduced area they occupy in discs when compared with wild-type *FRT40A* control clones. Area occupied by clones in 10 discs per genotype ($n = 10$) is represented in the graph. Horizontal lines indicate mean area. (C) Detail of a larva containing *FRT40A Tango1^{GS15095}* homozygous mutant hemocytes (blood cells) expressing cytoplasmic GFP as a marker and secreted RFP (*act>SPCg25C.RFP*). RFP accumulation in pericardial filter cells shows that *FRT40A Tango1^{GS15095}* mutant cells are capable of secretion.

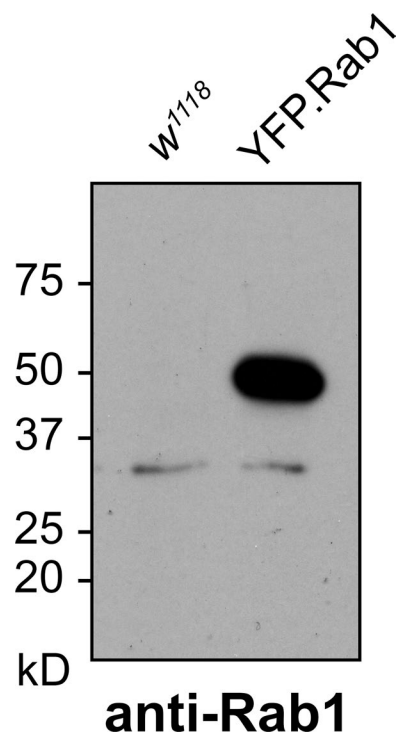


Figure S4. Anti-Rab1 antibody. Fat body lysates from wild-type and *Cg>YFP.Rab1* larvae were Western blotted with rabbit anti-Rab1 antibody generated in this study. YFP.Rab1 expression results in a strong band of higher molecular weight than endogenous, untagged Rab1.

Table S1. Predicted molecular mass of secreted proteins in this study

Proteins	Molecular mass
	kD
Vkg (Col IV α 2)	193.8
Cg25C (Col IV α 1)	174.3
Col IV trimer α 1 + α 2 + α 1	542.4
Rfabg (ApoB)	372.7
Trol (Perlecan)	316.8–496.9
Ndg (Nidogen)	149.1
Fat-spondin	84.9
Fer1HCH (Ferritin)	13.6–27.9
Hedgehog	52.1
Sgs3	32.2
VSVG	57.5
GFP/RFP/YFP	26.9

Table S2. Rescue of Tango1 knockdown by cytoplasmic Tango1

w ; Cg-GAL4 x w ; UAS-Tango1.RNA $i^{NIG11098R}$ / TM6B	w ; Cg-GAL4 ; UAS-GFP.Tango1 CYT x w ; UAS-Tango1.RNA $i^{NIG11098R}$ / TM6B
w ; Cg-GAL4 / + ; Tango1.RNA $i^{NIG11098R}$ / +	w ; Cg-GAL4 / + ; TM6B / GFP.Tango1 CYT
0	78
Number of adults and their genotype in the progeny of indicated crosses.	101
	87

Table S3. Experimental genotypes

Figure	Genotype
Fig. 1	Imaging of ERES–Golgi units through SIM microscopy
A–C	w ¹¹¹⁸
D	w ; Gmap ^{KM0132} .GFP
E	w ; Cg-GAL4 / + ; UAS-RFP.Rab1.3.1 / +
Fig. 2	Tango1 knockdown impairs general secretion in fat body cells
A	w ; vkg ^{G454} .GFP UAS-myr.RFP / + ; BM-40-SPARC-GAL4 / + w ; vkg ^{G454} .GFP UAS-myr.RFP / + ; BM-40-SPARC-GAL4 / UAS-PH4αEFB.RNAi ^{VDRCv2464} w ; vkg ^{G454} .GFP UAS-myr.RFP / + ; BM-40-SPARC-GAL4 / UAS-Tango1.RNAi ^{VDRC21594} w ; vkg ^{G454} .GFP UAS-myr.RFP / + ; BM-40-SPARC-GAL4 / UAS-PH4αEFB.RNAi ^{VDRCv2464} Tango1.RNAi ^{VDRC21594}
B	w ; vkg ^{G454} .GFP / + ; BM-40-SPARC-GAL4 / + w ; vkg ^{G454} .GFP / + ; BM-40-SPARC-GAL4 / UAS-Tango1.RNAi ^{VDRC21594}
C	w ; Cg-GAL4 / + ; UAS-Tango1.RNAi ^{VDRC21594} / +
D	w ; Cg-GAL4 / + ; UAS-SP ^{Vg} .RFP / + w ; Cg-GAL4 / + ; UAS-SP ^{Cg25C} .RFP / + w ; Cg-GAL4 / + ; UAS-SP ^{Vg} .RFP / UAS-Tango1.RNAi ^{VDRC21594} w ; Cg-GAL4 / + ; UAS-SP ^{Cg25C} .RFP / UAS-Tango1.RNAi ^{VDRC21594}
E	w ; Cg-GAL4 / + ; Rfabg.sGFP ^{TRG.900} / + w ; tro ^{CP1-002049} .YFP / w ; BM-40-SPARC-GAL4 UAS-myr.RFP / + w ¹¹¹⁸ w ; fat-spondin ^{CP1001685} .YFP / + ; BM-40-SPARC-GAL4 UAS-myr.RFP / + w ; Cg-GAL4 UAS-myr.RFP / + ; Fer1HCH ^{G188} .GFP / + w ; UAS-secr.GFP / + ; BM-40-SPA RC-GAL4 UAS-myr.RFP / + w ; Cg-GAL4 / + ; Rfabg.sGFP ^{TRG.900} / UAS-Tango1.RNAi ^{VDRC21594} w ; tro ^{CP1-002049} .YFP / w ; BM-40-SPARC-GAL4 UAS-myr.RFP / UAS-Tango1.RNAi ^{VDRC21594} w ; Cg-GAL4 / + ; UAS-Tango1.RNAi ^{VDRC21594} / + w ; fat-spondin ^{CP1001685} .YFP / + ; BM-40-SPA RC-GAL4 UAS-myr.RFP / UAS-Tango1.RNAi ^{VDRC21594} w ; Cg-GAL4 UAS-myr.RFP / + ; Fer1HCH ^{G188} .GFP / UAS-Tango1.RNAi ^{VDRC21594} w ; UAS-secr.GFP / + ; BM-40-SPARC-GAL4 UAS-myr.RFP / UAS-Tango1.RNAi ^{VDRC21594}
Fig. 3	Tango1 is widely expressed and required for secretion in salivary glands and disc cells
A	w ¹¹¹⁸
B	w ; Sgs3-GFP / + ; He-GAL4 UAS-myr.RFP / + w ; Sgs3-GFP / + ; He-GAL4 UAS-myr.RFP / UAS-Tango1.RNAi ^{VDRC21594}
C	w ; UAS-hh.GFP / + ; hh-GAL4 / + w ; UAS-hh.GFP / + ; hh-GAL4 / UAS-Tango1.RNAi ^{VDRC21594}
D	w ; UAS-secr.GFP / + ; rn-GAL4 / + w ; UAS-secr.GFP / + ; rn-GAL4 / UAS-Tango1.RNAi ^{VDRC21594}
Fig. 4	Tango1 differentially affects secretion of Collagen IV
A	w ; vkg ^{G454} .GFP / + ; UAS-SP ^{Vg} .RFP BM-40-SPARC-GAL4 / UAS-Tango1.RNAi ^{VDRC21594} w ; vkg ^{G454} .GFP / + ; UAS-SP ^{Vg} .RFP BM-40-SPA RC-GAL4 / UAS-Sec23.RNAi ^{VDRC24552GD} w ; vkg ^{G454} .GFP / + ; UAS-SP ^{Vg} .RFP BM-40-SPARC-GAL4 / UAS-Sar1.RNAi ^{VDRC34192GD}
B	w ; vkg ^{G454} .GFP UAS-myr.RFP / + ; BM-40-SPARC-GAL4 / + w ; UAS-secr.GFP / + ; BM-40-SPARC-GAL4 UAS-Dcr2 / + w ; Ub-VSVG.GFP / + ; BM40-SPARC-GAL4 UAS-myr.RFP / + w ; vkg ^{G454} .GFP UAS-myr.RFP / + ; BM-40-SPARC-GAL4 / UAS-Tango1.RNAi ^{VDRC21594} w ; vkg ^{G454} .GFP UAS-myr.RFP / + ; BM-40-SPARC-GAL4 / UAS-Sec23.RNAi ^{VDRC24552GD} w ; vkg ^{G454} .GFP UAS-myr.RFP / + ; BM-40-SPA RC-GAL4 / UAS-Sar1.RNAi ^{VDRC34192GD} w ; UAS-secr.GFP / + ; BM-40-SPARC-GAL4 UAS-Dcr2 / UAS-Sec23.RNAi ^{VDRC24552GD} w ; UAS-secr.GFP / + ; BM-40-SPARC-GAL4 UAS-Dcr2 / UAS-Sec23.RNAi ^{VDRC24552GD} w ; UAS-secr.GFP / + ; BM-40-SPARC-GAL4 UAS-Dcr2 / UAS-Sar1.RNAi ^{VDRC34192GD} w ; Ub-VSVG.GFP / + ; BM-40-SPARC-GAL4 UAS-myr.RFP / UAS-Tango1.RNAi ^{VDRC21594} w ; Ub-VSVG.GFP / + ; BM-40-SPARC-GAL4 UAS-myr.RFP / UAS-Sar1.RNAi ^{VDRC34192GD}
Fig. 5	Loss of Tango1 produces smaller ERES uncoupled from Golgi
A	w ; Cg-GAL4 / + ; Sec16.sGFP ^{TRG.1259} / + w ; Cg-GAL4 / + ; Sec16.sGFP ^{TRG.1259} / UAS-Tango1.RNAi ^{VDRC21594}
B	w ; Cg-GAL4 / + ; Sec16.sGFP ^{TRG.1259} / + w ; Cg-GAL4 / + ; Sec16.sGFP ^{TRG.1259} / UAS-Tango1.RNAi ^{VDRC21594}
C	y w ; Sec16.sGFP ^{TRG.1259} (y) w ; Tango1 ^{GS15095} ; Sec16.sGFP ^{TRG.1259}
D	w ; Cg-GAL4 UAS-Grasp65.GFP / + w ; Cg-GAL4 / + ; UAS-YFP.Rab1 / + w ; Cg-GAL4 UAS-Grasp65.GFP / + ; UAS-RFP.Rab1 / + w ; Cg-GAL4 UAS-Grasp65.GFP / + ; UAS-Tango1.RNAi ^{VDRC21594} / + w ; Cg-GAL4 / + ; UAS-YFP.Rab1 / UAS-Tango1.RNAi ^{VDRC21594} w ; Cg-GAL4 UAS-Grasp65.GFP / + ; UAS-RFP.Rab1.3.1 / UAS-Tango1.RNAi ^{VDRC21594}
E	w ; Cg-GAL4 / + ; Sec16.sGFP ^{TRG.1259} / UAS-Tango1.RNAi ^{VDRC21594} (anti-GM130) w ; Cg-GAL4 UAS-Grasp65.GFP / + ; UAS-Tango1.RNAi ^{VDRC21594} (anti-Sec16) w ; Cg-GAL4 / + ; UAS-YFP.Rab1 / UAS-Tango1.RNAi ^{VDRC21594} (anti-GM130) w ; Cg-GAL4 UAS-Grasp65.GFP / + ; UAS-RFP.Rab1.3.1 / UAS-Tango1.RNAi ^{VDRC21594} w ; Cg-GAL4 / + ; UAS-YFP.Rab1 / UAS-Tango1.RNAi ^{VDRC21594} (anti-Sec16)
Fig. 6	The cytoplasmic part of Tango1 directs ERES localization and can rescue Tango1 loss
C	w ; Cg-GAL4 / + ; UAS-GFP.Tango1 ^{CYT.3.1} / +
D	w ; Cg-GAL4 / + ; UAS-Tango1.RNAi ^{NIG11098R} / + w ; Cg-GAL4 / + ; UAS-GFP.Tango1 ^{CYT} / UAS-Tango1.RNAi ^{NIG11098R}
Fig. 7	Tango1 overexpression increases ERESs' size and number
A	w / Y OR y v sc ; ptc-GAL4 / UAS-Tango1.attP2
B	w ; Cg-GAL4 / + ; UAS-SP.GFP.Tango1.3.1 / + w ; Cg-GAL4 / + ; UAS-GFP.Tango1 ^{CYT.3.1} / + (30°C overexpression)
C	w ¹¹¹⁸ (anti-Tango1) w ; Cg-GAL4 / + ; UAS-SP.GFP.Tango1.3.1 / +
D	w ; Cg-GAL4 / + ; UAS-Tango1.RNAi ^{NIG11098R} / + (anti-Sec16) w ¹¹¹⁸ (fat body, anti-Tango1) w ; Cg-GAL4 / + ; UAS-SP.GFP.Tango1.3.1 / + w ¹¹¹⁸ (salivary gland, anti-Tango1)
E	w ¹¹¹⁸ (anti-Gmap) w ; Cg-GAL4 / + ; UAS-SP.GFP.Tango1.3.1 / + (anti-Gmap)
Fig. 8	Multiple interactions of Tango1 at the ERES–Golgi interface
A	w ; Cg-GAL4 ; UAS-Tango1.FLAG.3.1 UAS-Tango1.HA.3.1 w ; Cg-GAL4 ; UAS-Tango1.FLAG.3.1 w ; Cg-GAL4 ; UAS-Tango1.HA.3.1
B	w ; Cg-GAL4 ; UAS-Tango1.FLAG.3.1 w ¹¹¹⁸
C	w ; Cg-GAL4 ; UAS-YFP.Rab1 w ¹¹¹⁸
D	w ; Cg-GAL4 UAS-Grasp65.GFP w ¹¹¹⁸
E	w ; Cg-GAL4 ; UAS-Tango1.FLAG.3.1 w ¹¹¹⁸
F	w ; Cg-GAL4 ; UAS-YFP.Rab1 w ¹¹¹⁸
G	w ; Cg-GAL4 UAS-Grasp65.GFP w ¹¹¹⁸
H	y w ; Sar1 ^{CA07674} .GFP / TM3, Ser Sb w ¹¹¹⁸
Fig. S1	Efficiency of Tango1 knockdown

Table S3. Experimental genotypes (Continued)

Figure	Genotype
	$w^{1118} w ; Cg\text{-GAL4} / + ; UAS\text{-Tango1.RNAi}^{\text{VDRC21594}} / + w ; Cg\text{-GAL4} / + ; UAS\text{-Tango1.RNAi}^{\text{NG11098R}} / +$
Fig. S2	Overexpression of Collagen IV or Laminin single chains does not impair general secretion
	$w ; UAS\text{-secr.GFP} / + ; BM\text{-40-SPARC-GAL4 UAS-myR.RFP} / + w ; UAS\text{-secr.GFP} / + ; BM\text{-40-SPARC-GAL4 UAS-myR.RFP} / UAS\text{-Tango1.RNAi}^{\text{VDRC21594}} w ; UAS\text{-secr.GFP} / UAS\text{-Cg25C.RFP.2.1} ; BM\text{-40-SPARC-GAL4} / + w ; UAS\text{-secr.GFP} / + ; BM\text{-40-SPARC-GAL4} / UAS\text{-LanB1.RFP.3.1}$
Fig. S3	Analysis of Tango1 mutant mosaics
B	$y w ey\text{-Flp} ; FRT40A Tango1^{GS15095} / FRT40A y w ey\text{-Flp} ; FRT40A Tango1^{GS15095} / FRT40A tub\text{-GAL80} ; act\text{-y}\text{-GAL4 UAS-GFP} / + y w ey\text{-Flp} ; FRT40A / FRT40A tub\text{-GAL80} ; act\text{-y}\text{-GAL4 UAS-GFP} / + y w ey\text{-Flp} ; act\text{-y}\text{-GAL4 UAS-GFP} / + ; FRT82B Sar1^{11-3-63} / FRT82B tub\text{-GAL80} y w ey\text{-Flp} ; act\text{-y}\text{-GAL4 UAS-GFP} / + ; FRT82B / FRT82B tub\text{-GAL80}$
C	$w Pxn.B\text{-Flp.F12a} ; FRT40A Tango1^{GS15095} / FRT40A tub\text{-GAL80} ; act\text{-y}\text{-GAL4 UAS-GFP} / UAS\text{-SP}^{Cg25C}.RFP.3.1$
Fig. S4	Anti-Rab1 antibody
	$w^{1118} w ; Cg\text{-GAL4} ; UAS\text{-YFP.Rab1}$